PHYSICAL REVIEW B **95**, 184302 (2017)

Acoustic waves undetectable by transient reflectivity measurements

Chuan He,[1,2,3,*] Oliver Ristow,[1] Martin Grossmann,[1] Delia Brick,[1] Yuning Guo,[1] Martin Schubert,[1] Mike Hettich,[1] Vitalyi Gusev,[4] and Thomas Dekorsy[1,5]

[1]*Department of Physics, University of Konstanz, 78457 Konstanz, Germany*

[2]*Beijing Institute of Nanoenergy and Nanosystems, Chinese Academy of Sciences, Beijing 100083, China*

[3]*CAS Center for Excellence in Nanoscience, National Center for Nanoscience and Technology, Beijing 100190, China*

[4]*Laboratoire d'Acoustique de l'Université du Maine, LAUM, UMR, Centre National de la Recherche Scientifique 6613, 72085 Le Mans, France*

[5]*Institute of Technical Physics, German Aerospace Center (DLR), Pfaffenwaldring 38-40, 70569 Stuttgart, Germany*

(Received 16 February 2017; revised manuscript received 10 April 2017; published 11 May 2017)

A free-standing GaAs membrane is investigated by pump-probe reflectivity measurements with femtosecond laser pulses of 400-nm wavelength. It is found that the detected wide spectrum of laser-generated coherent strain waves in the membrane does not contain a specific hypersonic frequency. Theoretical analysis reveals that this effect is related to zero sensitivity of the acousto-optic detection at a particular frequency defined by the wavelength of the probe laser pulse on the mechanical free surface of the GaAs membrane. We predict that a similar behavior is expected in Si and Au membranes and films, indicating that the presence of zeros in the spectral transformation function of acousto-optic conversion is a rather general phenomenon in picosecond ultrasonics that has so far been neglected.

DOI: 10.1103/PhysRevB.95.184302

I. INTRODUCTION

Nanometer-thick planar phonon cavities have attracted much attention for investigating high-frequency acoustic phonons in the GHz to THz frequency range. Using time-resolved pump-probe laser spectroscopy, out-of-plane confined longitudinal coherent acoustic phonon (CAP) modes have been excited and detected in planar phonon cavities, such as supported films [1,2] and free-standing membranes [3–5]. For supported films, the laser-generated acoustic modes are coupled to a heat reservoir, thus the dynamics of the phonons in the film also depends on the acoustic parameters of the substrate. As a free-standing membrane is decoupled out of plane from any solid-state material, it has been proven to be a preferential model system for studying phononic properties of the individual materials. The membrane geometry has been employed to study the dynamics of coherent acoustic phonons in various semiconductors. In free-standing Si membranes, the mechanism for the generation and detection processes has been analyzed [3,4,6]. In addition, the relaxation of confined CAP modes has been investigated and the lifetime of the fundamental mode was obtained. Previously, confined CAP modes in a free-standing cubic GaN membrane were also investigated by femtosecond spectroscopy, and the ultrafast thickness oscillation of the membrane is observed and analyzed in the time domain [7]. As for GaAs, we published a first account on the observation of confined CAP modes in the free-standing GaAs membrane earlier in a review [5]; however, no detailed studies of the coherent acoustic pulses and vibrations in GaAs membranes have been reported until now.

In this paper, we describe the details of the preparation of the GaAs membranes, of the conducted experiments, and of the theoretical analysis, which provides an explanation of the "invisibility" of CAP at a specific hypersonic frequency in our experiments. We also analyze and discuss the generality of the revealed phenomenon of zero sensitivity of the transient optical reflectivity to CAP in picosecond laser ultrasonics of semiconductors and metals.

II. EXPERIMENTAL RESULTS

A free-standing [100] oriented GaAs membrane was prepared by cutting two trenches on the front side of the sample (GaAs epilayer/$Al_{0.5}Ga_{0.5}As$/GaAs substrate) using a focused ion beam and then immersing the sample in hydrofluoric acid (HF) solution to underetch the $Al_{0.5}Ga_{0.5}As$ layer with a thickness of 1 μm. The nominal thickness of the membrane is 200 nm. Figure 1 shows SEM images of as-fabricated membranes. Confined longitudinal CAP modes of the membrane are excited and detected by femtosecond pump-probe spectroscopy based on asynchronous optical sampling (ASOPS) [8,9]. All the measurements were performed in reflection geometry. The wavelength of 400 nm for both pump and probe laser pulses was obtained by frequency doubling of the initial pulses of 800 nm. The average powers for the pump and probe were 9 and 2 mW, respectively. Both beams were collinearly focused onto the sample at nearly normal incidence with a spot size of around 20 μm.

After subtracting the background unrelated to acousto-optic contribution to the reflectivity signal [Fig. 2(a-i)], the echo signals of the GaAs membrane, where a series of equally spaced echoes is seen, are shown in Fig. 2(a-ii). The background was subtracted by smoothing using the Savitzky-Golay method, where the points of window used is 800 and the polynomial order used is 2. Since the absorption depth of the light at 400 nm in GaAs is around 14 nm [10], the CAP pulse is generated and detected close to the surface of the GaAs membrane. The area illuminated by the laser beam, which determines the cross section of the generated acoustic beam, significantly exceeds the characteristic wavelengths of the CAPs, thus making diffraction effects negligible in the CAPs propagation. Hence, for the subsequent analysis of the

*hechuan@binn.cas.cn

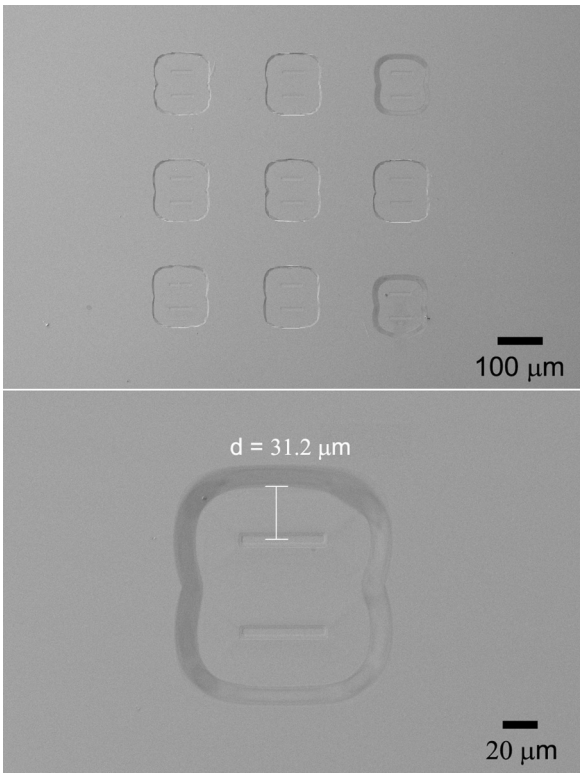

FIG. 1. SEM images of the GaAs membrane. Top: Array of nine membranes. Bottom: Single membrane with two trenches used for underetching of the GaAs film.

signals only the membrane motion perpendicular to its surface, i.e., in the z direction, is considered. Thus, the spacing between the adjacent echoes corresponds to the round-trip time, τ, of the strain pulse in the membrane and equals 80.4 ± 0.2 ps. Using this pulse-echo method and a speed of sound for GaAs of 4730 m/s in the [100] direction [11], the thickness of the membrane, d, is determined to be 190.1 ± 0.5 nm. Accounting for the fact that in the process of substrate etching the thickness of the layer is usually reduced relative to its grown thickness, this value is within 5% less compared to the nominal growth thickness of the membrane.

The fast Fourier transform (FFT) of the echoes is given in Fig. 2(b), where nearly equally spaced peaks are observed. These peaks correspond to the vibrational modes of the membrane. Due to the strong absorption of the light, both even and odd modes are generated and detected [5]. Figure 2(b) also compares the FFT results of the first and second echoes, which are indicated by solid and dashed gray lines, respectively. Both FFT spectra exhibit a double peak structure with two maxima at ∼60.0 and 120.0 GHz and a minimum at ∼93.6 GHz. In order to explain the discovered double peak structure of the detected pulse spectrum, we have taken into consideration the processes of generation, propagation, and detection of the CAPs by applying the theoretical methods developed in picosecond laser ultrasonics.

III. THEORY

The theoretical foundation of picosecond laser ultrasonics, a domain of research pioneered in the publications [12,13]

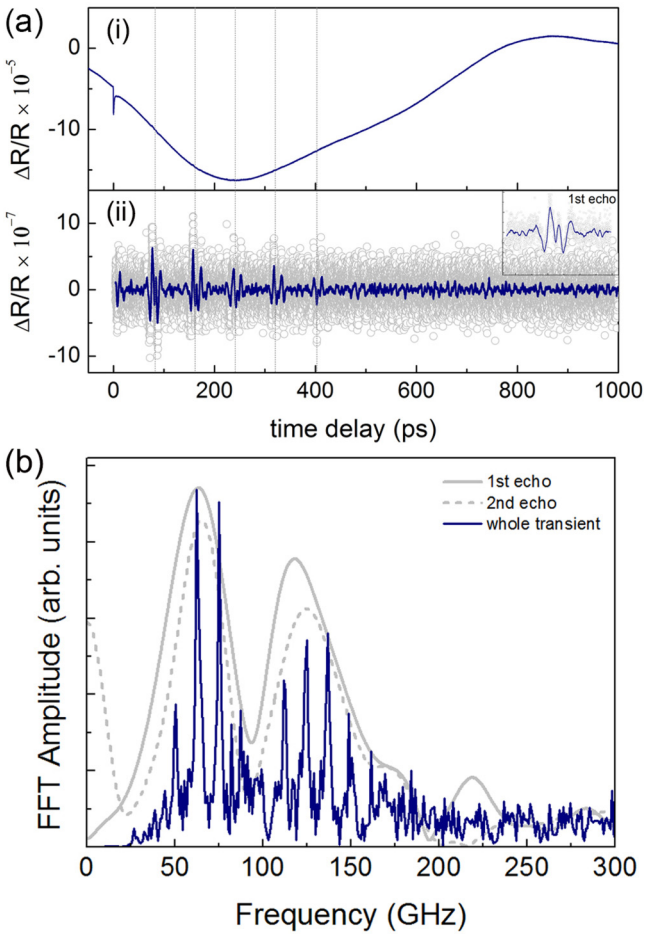

FIG. 2. (a-i) Transient background contribution to the reflectivity changes, which stems from the relaxation of photoexcited carriers, dynamics of the lattice temperature, and also contributions within the electronic circuit in phase with the repetition rate of the laser. (a-ii) Transient reflectivity change of the GaAs membrane after subtracting the background. The inset shows the first echo. The gray dots are the actual data, while the solid line is the smoothed curve shown for the purpose of better illustration of the pulses. (b) The FFT result of the echo signals and the comparison of the FFT results of the first (solid gray line) and second (dashed gray line) echo.

and dealing with application of all-optical generation and detection of hypersonic CAPs for fundamental studies and nondestructive testing of materials, was initially formulated in the time domain. Because in picosecond laser ultrasonics the generation of the acoustic waves through, for example, the thermoelastic effect is not delta localized at the surface of the materials but is distributed in depth near the laser-irradiated surface, generally an integral-type relation between the time profile of the pump laser pulse intensity envelope, $f(t)$, and the time profile of the emitted strain pulse, $\eta_{\text{emit}}(t)$, can be established [13,14]. Similarly, the detection of the strain waves through the acousto-optic effect takes place in the complete volume of probe light penetration and, as a consequence, in the time domain the acoustically induced changes in intensity of the reflected probe pulse, $dR(t)/R$, are also related to the time profile of the strain pulse, $\eta_{\text{inc}}(t)$, incident on the probed surface by an integral transformation [13,15].

Note that the time profile $\eta_{\text{emit}}(t)$ of the emitted pulse, which is by its definition propagating from the laser-irradiated surface, is introduced in laser optoacoustics from physical considerations at the shortest distance from the surface, $z = z_{\text{emit}}$, where the photoinduced stress is negligible [14]. The goal of this consists in splitting the description of the acoustic wave photoinitiation spatially into the domains of wave generation and of wave propagation. From the mathematics points of view the problem of solving the inhomogeneous wave equation in the full space is divided into two successive problems. The first one, the "generation problem," is to solve the inhomogeneous wave equation in the domain $0 < z < z_{\text{emit}}$. The second one, the "propagation problem," is to solve the homogeneous wave equation, i.e., neglecting photoinduced stress in the rest of the space using as a boundary condition the solution of the first problem at $z = z_{\text{emit}}$. This approach provides important simplifications for the description of most of the experimental situations (including our experiments described above), because in the picosecond laser ultrasonics experiments the characteristic lengths of the acoustic wave attenuation and dispersion are commonly much longer than the depth of the photoinduced stress localization. This separation of spatial scales provides the opportunity (i) to neglect the attenuation and dispersion, when solving the inhomogeneous wave equation in the domain $0 < z < z_{\text{emit}}$, and (ii) to replace approximately its solution at $z = z_{\text{emit}}$ by the formal solution of the same simplified equation at infinitely large distances. In other words, the emitted acoustic pulse at $z = z_{\text{emit}}$ is found as the solution at infinite distances from the surface of the inhomogeneous equation for the nondispersive and nonattenuated waves in a half space [14,16]. Similarly, in many experimental configurations, including our experiments described above, the penetration depth of the probe laser light can be much shorter than the characteristic lengths of attenuation and dispersion of the photogenerated acoustic pulses. In this case, it is advantageous to determine the profile of the acoustic strain pulse approaching the optically probed surface, $\eta_{\text{inc}}(t)$, at the minimal distance from this surface, $z = z_{\text{inc}}$, where the probe laser field is negligible. The strain pulse at $z = z_{\text{inc}}$ can be found from the solution of the propagation problem, defined above, while in the region probed by the optical radiation its propagation can be considered as nonattenuated and nondispersive. In this case, the profile of the pulse approaching the optically probed surface is the same at $z = z_{\text{inc}}$ and 0, and $\eta_{\text{inc}}(t)$ can be equivalently defined at $z = 0$. Note that in our experimental configuration the propagation path of the photogenerated pulse from $z = z_{\text{emit}}$ to $z = z_{\text{inc}}$ includes its reflection at the mechanically free surface of the membrane.

The method of spectral transformation functions, initially developed for laser ultrasonics [14], was first applied in picosecond laser ultrasonics in Refs. [16,17] and later proved its efficiency for the analysis of various experimental configurations [16,18–21]. In the frequency domain the spectrum of the emitted acoustic pulse, $\tilde{\eta}_{\text{emit}}(\omega)$, and the spectrum of the pump laser pulse intensity envelope, $\tilde{f}(\omega)$, have a linear relationship and can be written as follows:

$$\tilde{\eta}_{\text{emit}}(\omega) = K_{\text{OA}}(\omega) I_{\text{pump}} \tilde{f}(\omega) \cong K_{\text{OA}}(\omega) F_{\text{pump}}, \qquad (1)$$

where $K_{\text{OA}}(\omega)$ is the spectral transformation function of the optoacoustic conversion while I_{pump} and F_{pump} are the peak intensity and the fluence of the pump laser pulse, respectively. $K_{\text{OA}}(\omega)$ describes the efficiency of conversion of each particular frequency from the laser pulse intensity envelope into the same frequency of the acoustic pulse spectrum. $K_{\text{OA}}(\omega)$ depends not only on the parameters of the material and of the pump laser radiation but also on the acoustic boundary conditions at the laser irradiated surface/interface [14]. Since the approximate relation in Eq. (1) is independent of the laser pulse intensity envelope spectrum and contains only the constant pump laser fluence, it is very precise for the sub-picosecond and femtosecond pump laser pulses with the negligible variations of $\tilde{f}(\omega)$ below 1 THz, i.e., in the hypersound frequency range of interest here. Although the opportunity to describe the detection of CAPs in the frequency domain had been noticed already in Ref. [15], it was applied for the first time to the analysis of the experiments quite recently [20] and only for a particular case of CAPs detection near the interface of transparent and opaque solids. In general, in the frequency domain the relation between the spectrum of the transient reflectivity, $d\tilde{R}(\omega)/R$, detected by probe pulse of sub-picoseconds-femtoseconds duration and the spectrum of the acoustic strain pulse incident on the probed surface/interface, $\tilde{\eta}(\omega)$, is a linear algebraic one:

$$d\tilde{R}(\omega)/R = K_{\text{AO}}(\omega)\tilde{\eta}_{\text{inc}}(\omega) \qquad (2)$$

where the spectral transformation function of the acousto-optic conversion, $K_{\text{AO}}(\omega)$, depends on the parameters of the material, on the parameters of probe laser radiation, and also on the acoustic boundary conditions at the laser probed surface/interface [15,20]. $K_{\text{AO}}(\omega)$ characterizes the efficiency of conversion of each particular frequency from the spectrum of a coherent strain pulse into the spectrum of a transient reflectivity.

Likewise, the transformation of the acoustic pulse caused by its propagation can be conveniently described in the frequency domain by

$$\tilde{\eta}_{\text{inc}}(\omega) = K_{\text{AA}}(\omega)\tilde{\eta}_{\text{emit}}(\omega). \qquad (3)$$

Here the spectral transformation function of acousto-acousto conversion, $K_{\text{AA}}(\omega)$, associates with the potential effects that accompany acoustic pulse propagation, such as attenuation (including absorption and scattering), dispersion, diffraction, and reflections at surfaces/interfaces [14,16]. Combining Eqs. (1)–(3) we derive the following relation:

$$d\tilde{R}(\omega)/R = K_{\text{AO}}(\omega)K_{\text{AA}}(\omega)K_{\text{OA}}(\omega)F_{\text{pump}}. \qquad (4)$$

This relation indicates that the experimentally revealed zero in the detected spectrum, $d\tilde{R}(\omega)/R$, of the transient reflectivity could be potentially related to the zero in one of the defined spectral transformation functions.

In theory, neither dispersion nor diffraction phenomena can completely eliminate a particular finite frequency component in the spectrum of the propagating strain pulse. Potentially a formation of a pronounced minimum in $K_{\text{AA}}(\omega)$ could be caused by some resonant processes of absorption or scattering in the bulk or at the surfaces/interfaces. However, the absence of any resonant CAPs attenuation in the frequency range around 100 GHz of interest here has been theoretically

previewed based on the experimental results for hypersound absorption in GaAs [22,23], thus the presence of zero in $K_{\mathrm{AA}}(\omega)$ at some finite hypersonic frequency can be excluded.

The spectral transformation function $K_{\mathrm{OA}}(\omega)$ for sound generation by a femtosecond laser pulse at 400 nm in GaAs was derived in Ref. [21], and it was successfully applied to explain the experimental observations afterwards. For our experimental conditions, it is possible to demonstrate analytically that $K_{\mathrm{OA}}(\omega)$ does not contain zeros or pronounced minima at finite hypersonic frequencies, and this can also be confirmed by direct numerical evaluation. Moreover, we verified that the inclusion of the surface recombination of the photogenerated charge carriers [14,16] and the optoacoustic conversion via the thermoelastic mechanism [16,21] does not introduce zeros or pronounced minima in $K_{\mathrm{OA}}(\omega)$ at finite hypersonic frequencies. Theoretically, for the disappearance of a particular frequency in optoacoustic conversion, the materials and structures of at least two optoacoustic conversion mechanisms operating in antiphase are advantageous, such as the deformation potential and thermoelasticity both operating in silicon [14,15,24] and the deformation potential in a silicon membrane combined with thermoelasticity of metallic thin film deposited on it [5,25]. In these cases the photoexcitation of electron-hole pairs near the lowest indirect energy gap of silicon causes its contraction, while heating of either silicon or metal usually leads to its expansion. However, in GaAs the deformation potential of electron-hole pairs near the fundamental energy gap operates in phase with thermoelasticity [16,26], and furthermore at the low pump laser fluence compared to those in Ref. [21] the thermoelastic contribution to the total photogenerated strain pulse is largely negligible [16,17,21,26].

The zero efficiency in optoacoustic transformation could also take place in materials with a single physical mechanism of the conversion, which operates with different phases through several channels. In our case, where the pump laser pulse with a wavelength of 400 nm incidents on the GaAs surface, the initially photoexcited electrons first relax at sub-pico-second time scale to higher-energy conduction valleys X and L and later relax to the lowest conduction valley in the Γ point [27–30]. There are indications in the literature that the sign of the electron phonon deformation at least in a part of the higher-energy valleys could be opposite to its sign in the Γ valley [11]. Thus, the electrons in the higher and in the lowest valleys could potentially generate CAPs in antiphase. However, it is well established that the relaxation of the electrons from the higher valleys to the lowest one takes place faster than in $\tau_{\mathrm{rel}} \leqslant 1$ ps [27–30]. Because of this finite lifetime of the nonequilibrium electrons in higher conduction bands, the spectrum of CAPs generated is expected to have a low-frequency cutoff at around $f = \omega/(2\pi) \geqslant 1/(2\pi\tau_{\mathrm{rel}}) \propto$ 160 GHz [14,24]. This preliminary and qualitative theoretical analysis indicates that hypothetical compensation of two different channels of the deformation potential mechanism cannot lead to zero in $K_{\mathrm{OA}}(\omega)$ at the frequency of ∼93.6 GHz [see Fig. 2(b)], because the generation of the CAPs by higher valley electrons is strongly suppressed at this frequency. Although the quantitative analysis of possible compensation of two deformation potential mechanism channels in GaAs is of general interest in our opinion, we are not developing it in this paper because we have found the main reason for the zero in the detected spectrum of the transient reflectivity as discussed below. In the following paragraph we will prove that the pronounced minimum at ∼93.6 GHz in the detected spectrum of the transient reflectivity of 400-nm probe light is caused by the zero in the sensitivity of the acousto-optic conversion in GaAs, i.e., by the zero in $K_{\mathrm{AO}}(\omega)$.

To derive the spectral transformation function of the acousto-optic conversion, $K_{\mathrm{AO}}(\omega)$, we started by rewriting the theoretical formula for the transient reflectivity, $dR(t)/R$, in the time domain from Ref. [13], where the probe light is incident on the interface of the material with air (vacuum), in terms of the material dielectric function:

$$\frac{dR(t)}{R} = -4k_0\mathrm{Re}\left\{i\frac{\partial\varepsilon/\partial\eta}{\varepsilon-1}\int_0^{\infty}\eta(z,t)e^{2ik_0\sqrt{\varepsilon}z}dz\right\}, \quad (5)$$

where R is the reflection coefficient for optical intensity, $k_0 = 2\pi/\lambda_0$ is the probe wave in vacuum, Re stands for the real part of the complex function, $\varepsilon = \varepsilon' + i\varepsilon''$ is the complex dielectric function, $\partial\varepsilon/\partial\eta = \partial\varepsilon'/\partial\eta + i\partial\varepsilon''/\partial\eta$ is the complex acousto-optic coefficient, and $\eta(z,t)$ is the coherent strain field distribution in the sample region, along the z axis normal to the surface, detected by the probe laser field. The theoretical formula in Eq. (5) is valid near a mechanically free surface of the material as the loading by air is negligible. Consequently the probed strain field $\eta(z,t)$ can be decomposed into two strain pulses traveling with the acoustic velocity c_a: the strain pulse $\eta_{\mathrm{inc}}(t + z/c_a)$ incident on the surface $z = 0$ from the bulk and the reflected strain pulse $\eta_{\mathrm{ref}}(t - z/c_a) = -\eta_{\mathrm{inc}}(t - z/c_a)$, where the sign "−" in front of the right-hand side accounts for the strain sign inversion in reflection from the mechanically free surface [15]:

$$\begin{aligned}\eta(t,z) &= \eta_{\mathrm{inc}}(t + z/c_a) - \eta_{\mathrm{inc}}(t - z/c_a)\\ &= \frac{1}{2\pi}\int_{-\infty}^{+\infty}\tilde{\eta}_{\mathrm{inc}}(\omega)e^{-i\omega t}[e^{-ik_a z} - e^{ik_a z}]d\omega, \quad (6)\end{aligned}$$

where $k_a = \omega/c_a$ is the wave number of CAP.

By substitution of Eq. (6) into Eq. (5) we can do the integration over the spatial coordinate z:

$$\frac{dR(t)}{R} = \frac{1}{2\pi}\left\{8k_0\mathrm{Re}\left[\frac{\partial\varepsilon/\partial\eta}{\varepsilon-1}\int_{-\infty}^{+\infty}\frac{k_a}{(2k_0)^2\varepsilon - k_a^2}\tilde{\eta}_{\mathrm{inc}}(\omega)e^{-i\omega t}d\omega\right]\right\}. \quad (7)$$

Taking into account that the strain field is real, thus $\tilde{\eta}_{\mathrm{inc}}(-\omega) = \tilde{\eta}^*_{\mathrm{inc}}(\omega)$, where "∗" denotes complex conjugation, also neglecting CAPs attenuation in their propagation through the optically probed region, i.e., assuming real acoustical wave numbers, Eq. (7) can be transformed to the following form:

$$\frac{dR(t)}{R} = \frac{1}{2\pi}\left\{-4i\int_{-\infty}^{+\infty}\bar{k}_a(\omega)\mathrm{Im}\left[\frac{\partial\varepsilon/\partial\eta}{(\varepsilon-1)[\varepsilon - \bar{k}_a(\omega)]}\right]\tilde{\eta}_{\mathrm{inc}}(\omega)e^{-i\omega t}d\omega\right\}, \quad (8)$$

where $\bar{k}_a(\omega) = k_a(\omega)/(2k_0)$ is the normalized acoustic wave number. At the same time, using the definitions of the Fourier transform and of the spectral transformation function of the acousto-optic conversion, $K_{AO}(\omega)$, in Eq. (2), $dR(t)/R$ can be presented as

$$\frac{dR(t)}{R} = \frac{1}{2\pi}\int_{-\infty}^{+\infty}\frac{d\tilde{R}(\omega)}{R}e^{-i\omega t}d\omega = \frac{1}{2\pi}\int_{-\infty}^{+\infty}K_{AO}(\omega)\tilde{\eta}_{inc}(\omega)e^{-i\omega t}d\omega. \quad (9)$$

Comparing Eq. (8) with Eq. (9) provides the solution for $K_{AO}(\omega)$:

$$K_{AO}(\omega) = -4i\bar{k}_a(\omega)\mathrm{Im}\left\{\frac{\partial\varepsilon/\partial\eta}{(\varepsilon-1)\left[\varepsilon-\bar{k}_a^2(\omega)\right]}\right\}. \quad (10)$$

For evaluating the amplitude spectrum of transient reflectivity, the modulus of the spectral transformation function $K_{AO}(\omega)$ can be written in the form

$$|K_{AO}(\omega)| = \frac{4|a|}{(\varepsilon'-1)^2+\varepsilon''^2}\left\{\frac{\bar{k}_a(\omega)\left|\varepsilon'+(b/a)\varepsilon''-\bar{k}_a^2(\omega)\right|}{\left[\varepsilon'-\bar{k}_a^2(\omega)\right]^2+\varepsilon''^2}\right\}, \quad (11)$$

where the following notations are introduced: $a = \varepsilon''\partial\varepsilon'/\partial\eta - (\varepsilon'-1)\partial\varepsilon''/\partial\eta$ and $b = (\varepsilon'-1)\partial\varepsilon'/\partial\eta + \varepsilon''\partial\varepsilon''/\partial\eta$. Note that the dependence of $|K_{AO}(\omega)|$ on the frequency of CAPs is only due to the dependence on frequency of the CAP wave number, $\bar{k}_a(\omega) \propto \omega$. Because of this asymptotic behavior of $|K_{AO}(\omega)|$, we have $|K_{AO}(\omega)| \propto |\omega|$ and $1/|\omega|$ at lowest and highest frequencies, respectively. It is also worth noting that Eq. (9) correctly predicts that in the case of a nearly transparent material the highest efficiency of the acousto-optic transformation is due to a synchronous process of the Brillouin backscattering taking place for the acoustic wave numbers satisfying the condition $\bar{k}_a^2(\omega) = \varepsilon'$, a more familiar form of which is $k_a(\omega) = 2k_0 n$, where n denotes the optical refractive index. However, for our present research the prediction by Eq. (9) of a possible zero in $|K_{AO}(\omega)|$ at finite acoustic frequency is of primary importance. The spectral transformation function could be potentially equal to zero only if the condition $\varepsilon' + (b/a)\varepsilon'' > 0$ is fulfilled. Under the above condition, the acoustic frequency, which is undetectable by transient optical reflectivity, has the following theoretical expression:

$$f_0 = \frac{c_a k_0}{\pi}\sqrt{\varepsilon'+\frac{b}{a}\varepsilon''} = \frac{c_a k_0}{\pi}\sqrt{\frac{(2\varepsilon'-1)\varepsilon''\partial\varepsilon'/\partial\eta - [\varepsilon'(\varepsilon'-1)-\varepsilon''^2]\partial\varepsilon''/\partial\eta}{\varepsilon''\partial\varepsilon'/\partial\eta - (\varepsilon'-1)\partial\varepsilon''/\partial\eta}}. \quad (12)$$

In order to evaluate the theoretically predicted f_0 under our experimental conditions (GaAs with the z axis oriented along [100], $\lambda_0 = 400$ nm) we have used the dielectric constant $\varepsilon \cong 14.5 + i18.8$ from Refs. [10,31], estimated the photoelastic constants $P_{11} \cong (7.1 + i3.1)$ GPa^{-1} and $P_{12} \cong -(3.8 + i0.029)$ GPa^{-1} using Fig. 3 from Ref. [31], and derived the required acousto-optic constants $\partial\varepsilon/\partial\eta \cong -278.0 + i162.5$ using the relation $\partial\varepsilon/\partial\eta \cong P_{11}C_{11} + P_{12}(C_{11}+C_{12})$ and real elastic moduli of GaAs, $C_{11} \cong 119.0$ GPa and $C_{12} \cong 53.4$ GPa [32]. The CAPs in our experimental geometry contain a single component of the strain tensor $\varepsilon_{zz} \equiv \varepsilon_{33}$ and propagate with the velocity $c_a \cong 4730$ m/s. Substituting the above listed parameters in Eq. (10) provides the theoretical estimate for the undetectable frequency, f_0^{theor}(GaAs,400 nm) ≈ 95.5 GHz, which is in a very good agreement with the position of the experimentally observed pronounced minimum in the amplitude spectrum of the detected CAPs [Fig. 2(b)]. In the next section we will demonstrate that the existence of the acoustic frequencies undetectable by transient reflectivity measurements in picosecond laser ultrasonics is a rather general and widely spread phenomenon. This should be taken into consideration when choosing a material and an optical probe wavelength for monitoring CAPs in a particular frequency range.

IV. DISCUSSION

Using Eqs. (11) and (12) and the parameters of GaAs available in the literature [10,31,33] the dependences of f_0^2 and $|K_{AO}(\omega)|$ on the probe optical wavelength are shown in Figs. 3(a) and 3(b), respectively. Obviously, the undetectable frequencies exist only for positive values of $(f_0)^2$. Figure 3(a) demonstrates that the undetectable frequencies exist in the large bands of probe wavelengths, while all CAP frequencies can be potentially detected only in narrow bands of the wavelengths near the well-known critical points E_1, $E_1 + \Delta_1$, and E_2 of the joint density of states associated with the optical transitions in GaAs [11,34–36] at probe wavelengths around 429 nm (2.9 eV), 397 nm (3.13 eV), and 264 nm (4.7 eV), respectively [35]. Figure 3(b) demonstrates that in GaAs the detection of hypersound in large frequency bands extending up to several hundreds of GHz is possible using short optical wavelengths ($\leqslant 440$ nm), although it can be importantly distorted by the effect of zero acousto-optic sensitivity [see $K_{AO}(\omega)$ for the 400-, 395-, and 302-nm probe wavelengths in Fig. 3(b), for example]. At longer probe wavelengths the detection becomes more and more narrow band and concentrated around the Brillouin frequency [see Fig. 3(b) for 495 nm as an example].

Silicon is another semiconductor with the documented photoelastic parameters. Accounting for Eqs. (11) and (12) and using the parameters of Si from the literature [10,37], the dependences of f_0^2 and $|K_{AO}(\omega)|$ on probe optical wavelength are evaluated and presented in Figs. 4(a) and 4(b), respectively. These figures confirm the presence of the undetectable frequency in an extremely large band of probe wavelengths in Si. It is to note that using acousto-optic constants documented in Refs. [10,37,38] for the probe wavelength around 440 nm, the undetectable acoustic frequencies could exist (red dot, Ref. [38]) or do not exist (dot shaded by the gray square, Ref. [37]). The increase of the f_0 in Si and its transition to the THz region at probe wavelengths approaching 290–277 nm could be correlated to the optical critical point E_2 in the band structure at 4.27–4.49 eV [39]. The features similar to those illustrated in Figs. 3 and 4 in semiconductors

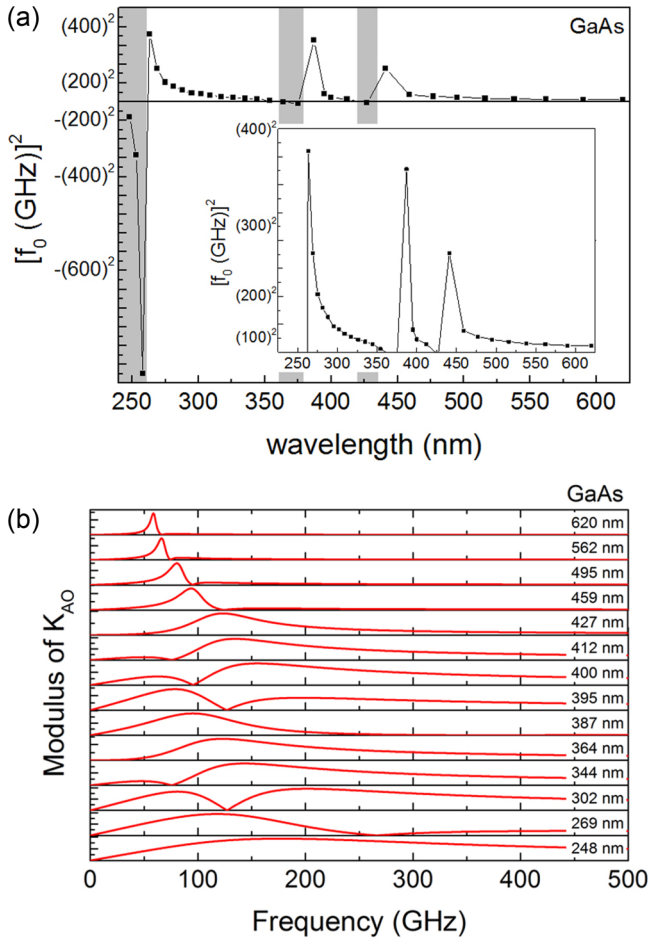

FIG. 3. (a) The dependence of the square of the acoustic frequency, f_0^2, on the optical wavelength of probe light from 248 to 620 nm in GaAs. The positive values of f_0^2 provide real valued undetectable frequencies f_0. The areas shaded in gray correspond to the probe wavelengths at which all acoustic frequencies are detectable. The inset shows the dependence of the positive values of f_0^2 on the optical wavelength. (b) The modulus of the spectral transformation function of acousto-optic conversion at the mechanically free surface of GaAs for different wavelengths of probe light, varying from 248 to 620 nm. All the local minima in the modulus of $K_{AO}(\omega)$ correspond to undetectable acoustic frequencies. With increasing wavelength of the probe beam the detection sensitivity is progressively concentrating around the Brillouin frequency in backscattering configuration.

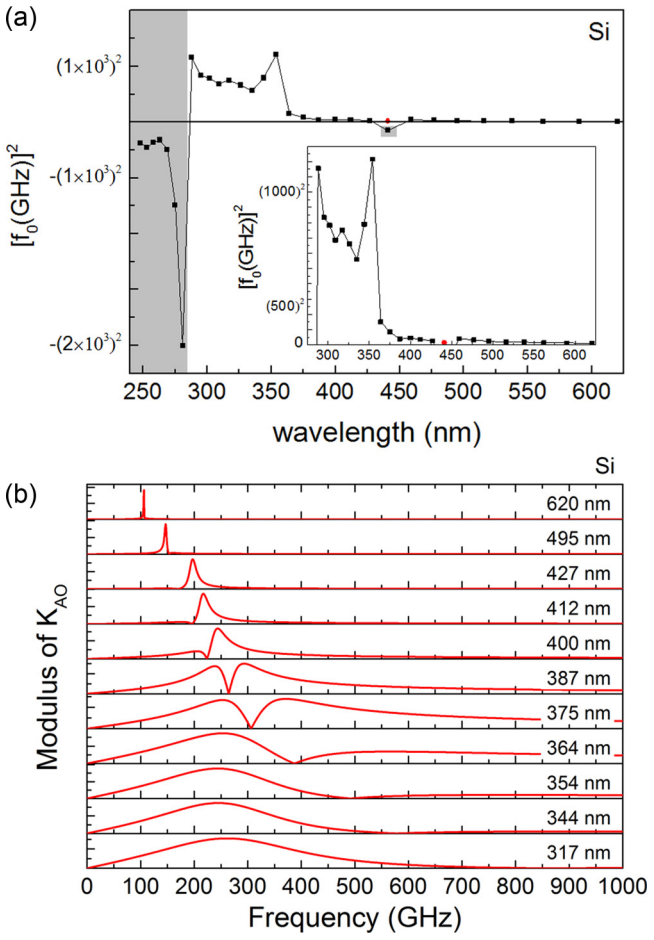

FIG. 4. (a) The dependence of the square of the acoustic frequency, f_0^2, on the optical wavelength of probe light from 317 to 620 nm in Si. The positive values of f_0^2 provide real valued undetectable frequencies f_0. The areas shaded in gray correspond to the probe wavelengths at which all acoustic frequencies are detectable. The inset shows the dependence of the positive values of f_0^2 on the optical wavelength. For the probe wavelength around 440 nm, the undetectable acoustic frequencies could exist (red dot, Ref. [38]) or do not exist (dot shaded by gray square, Ref. [37]) depending on the acousto-optic constants used. (b) The modulus of the spectral transformation function of acousto-optic conversion at the mechanically free surface of Si for different wavelengths of probe light, varying from 317 to 620 nm. All the local minima in the modulus of $K_{AO}(\omega)$ correspond to undetectable acoustic frequencies. With increasing wavelength of the probe beam the detection sensitivity is progressively concentrating around the Brillouin frequency in backscattering configuration.

could be also expected in the vicinity of the so-called parallel band optical interband absorption regions in metals. In Fig. 5, as an example, we present the results of the evaluation of the zero sensitivity frequency in Au, using the data on the optical and acousto-optical parameters of this metal reported in Refs. [40,41], respectively. The analysis of the results presented in Fig. 5 demonstrates that, similar to the cases of semiconductors, GaAs and Si, presented above, the principle changes in the spectral transformation function of the optoacoustic conversion, from the viewpoint of existence/inexistence of undetectable acoustic frequencies, are taking place in the vicinity of the maxima in the electron density of states (DOS) for the optical transitions. In the case of Au, these transitions are from three local maxima in the density of the states in the broad electron d band towards the nonoccupied levels in the vicinity of the Fermi level of the electron conduction s/p band [42,43]. However, the theoretical prediction for Au in Fig. 5 is drastically different from those for GaAs and Si in Figs. 3(a) and 4(a), respectively. In semiconductors the zero sensitivity frequency disappears in the vicinity of the maxima in the joint DOS associated with the optical transitions, while in Au the zero frequency appears only near the maxima in the joint DOS associated with the optical transitions and does not exist in most parts of the analyzed probe light spectrum.

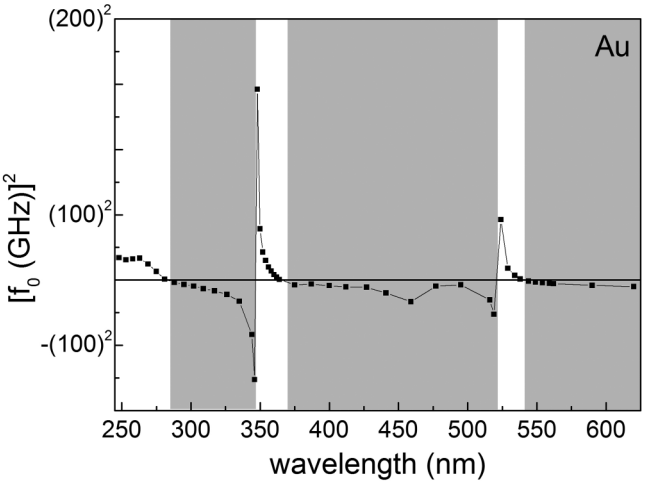

FIG. 5. The dependence of the square of the acoustic frequency, f_0^2, on the optical wavelength of probe light from 248 to 620 nm in Au. The positive values of f_0^2 provide real valued undetectable frequencies f_0. The areas shaded in gray correspond to the probe wavelengths at which all acoustic frequencies are detectable.

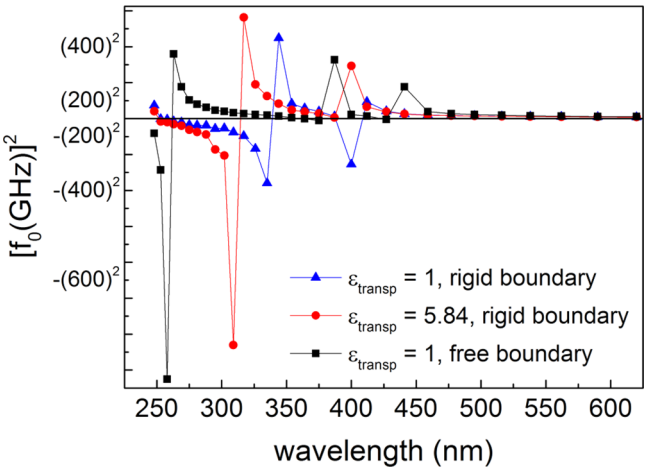

FIG. 6. The dependence of the square of the acoustic frequency, f_0^2, on the optical wavelength of probe light in the case of the acousto-optic detection of hypersound in GaAs substrate loaded by the media with different acoustic and electromagnetic properties. Triangles stand for loading by a hypothetical absolutely rigid material with electromagnetic properties of vacuum. Circles correspond to the case where the optical properties of the absolutely rigid material are those of diamond. Squares depict the results for loading of the GaAs surface by air. Undetectable real valued acoustic frequencies f_0 exist at such wavelengths of probe light for which f_0^2 is positive. The existence or inexistence of the acoustic frequencies undetectable through the acousto-optic effect for a particular wavelength of probe light, incident on the interface between the transparent and opaque media, depends both on the mechanical and electromagnetic boundary conditions at the interface.

From the theoretical analysis and the discussion above it follows that the presence of the nondetectable hypersonic frequency is a rather common effect in CAPs detection by transient reflectivity technique, while its absence corresponds to particular probe wavelengths in the vicinity of the specific critical points of the materials band structure. However, it should be kept in mind that the theoretical expression for the zero sensitivity frequency f_0 in Eq. (12) has been derived assuming a mechanically free surface of the tested samples. In general, similar to the spectral transformation function of optoacoustic conversion [14], $K_{OA}(\omega)$, the spectral transformation function of acousto-optic conversion, $K_{AO}(\omega)$, depends on the boundary conditions for the CAPs transmission through and reflection from the optically probed interface [20]. Below, to illustrate this point, we evaluated the zero sensitivity frequency, for the interface between the probed opaque material and an absolutely elastically rigid and absolutely optically transparent one. In this hypothetical situation the dielectric parameter of the opaque material, ε, should be replaced in the equations starting Eq. (5) by its value normalized to the real dielectric constant of the transparent material, $\varepsilon \Rightarrow \bar{\varepsilon} \equiv \varepsilon/\varepsilon_{transp}$, $k_0 \Rightarrow k_{transp}$, and it is necessary to account for the change of the CAPs reflection coefficients at the interface by modifying the reflected strain wave as follows: $\eta_{ref}(t - z/c_a) = \eta_{inc}(t - z/c_a)$. These modifications lead to the solution for the zero sensitivity frequency at the rigid interface, $f_0^{rigid} = f_0[a(\varepsilon) \Rightarrow b(\bar{\varepsilon}), b(\varepsilon) \Rightarrow -a(\bar{\varepsilon})]$, that can be rewritten in the form

$$f_0^{rigid} = \frac{c_a k_0}{\pi} \sqrt{\frac{[\varepsilon'(\varepsilon' - \varepsilon_{transp}) - \varepsilon''^2]\partial\varepsilon'/\partial\eta + (2\varepsilon' - \varepsilon_{transp})\varepsilon''\partial\varepsilon''/\partial\eta}{(\varepsilon' - \varepsilon_{transp})\partial\varepsilon'/\partial\eta + \varepsilon''\partial\varepsilon''/\partial\eta}}. \quad (13)$$

In Fig. 6 we present the results of the evaluation of f_0^{rigid} for GaAs in the cases of $\varepsilon_{transp} = 1$ (hypothetical absolutely rigid optical vacuum, blue triangles) and $\varepsilon_{transp} = 5.84$ (diamond, red dots). For the convenience of comparison we also present the results for the mechanically free surface from Fig. 3. Figure 6 demonstrates that the predicted "invisible" frequencies depend both on the reflection at the interface of the CAPS and on transmission/reflection at the interface of the probe light. The existence or inexistence of the acoustic frequencies undetectable through the acousto-optic effect for a particular wavelength of probe light, incident on the interface between the transparent and opaque media, depends both on the mechanical and electromagnetic boundary conditions at the interface. These predictions also indicate that, in general, the derived theoretical formulas cannot be applied straightforwardly for the analysis of the experimental results in the cases of free-standing membranes and thin films deposited on the substrates at such optical wavelengths at which the membranes/films are not completely opaque. For these cases the theory should be modified by taking into account multiple reflections of the probe light inside the membrane/film.

It is also worth discussing the application of the picosecond laser ultrasonics for determining the ratio of the acousto-optic constants $\partial\varepsilon'/\partial\eta$ over $\partial\varepsilon''/\partial\eta$. In the so-called colored picosecond laser ultrasonics [44–48], where the transient reflectivity measurements are conducted with wavelength-tunable probe laser pulses, and in the experiments conducted at a single probe wavelength [26,49–51] either the ratio of $\partial\varepsilon'/\partial\eta$ over $\partial\varepsilon''/\partial\eta$ or the related ratio of $\partial n'/\partial\eta$ over $\partial n''/\partial\eta$ is commonly determined by fitting the detected profiles of the strain pulses to the theoretically predicted ones. Our analysis presented above indicates that potentially this ratio could be obtained from the measured zero in the spectral transformation function, $K_{\mathrm{AO}}(\omega)$. By inverting Eq. (12), we predict

$$\frac{\partial\varepsilon'/\partial\eta}{\partial\varepsilon''/\partial\eta} = \frac{(\varepsilon'-1)\bar{k}_a^2 - [\varepsilon'(\varepsilon'-1)-\varepsilon''^2]}{\varepsilon''\bar{k}_a^2 - (2\varepsilon'-1)\varepsilon''}. \tag{14}$$

In Eq. (14) the normalized acoustic wave number should be evaluated for the experimentally detected frequency of the zero in the acoustic spectrum. Equation (14) has been applied to determine the ratio of the acousto-optic coefficient from our experimentally determined $f_0^{\mathrm{exp}} = 93.6$ GHz. The obtained ratio of -1.6 is in reasonable agreement with one, i.e., -2.2, that could be derived at 400 nm from the data reported in Ref. [31], taking into account that in Ref. [31] there are no data precisely at 499 nm and the extrapolation of the data for other wavelengths is necessary, which could be rather imprecise.

V. CONCLUSION

To summarize, a free-standing GaAs membrane is prepared and investigated by femtosecond pump-probe spectroscopy based on the ASOPS technique. Due to the short absorption depth of the light at 400 nm, the excitation of the GaAs membrane generates a strain pulse that propagates in the sample. The detected echo signal has a double peak structure in the frequency domain. Our analysis shows that this is mainly caused by the double peak structure of the spectral transformation function of acousto-optic conversion, $K_{\mathrm{AO}}(\omega)$. This approach reproduces the main observations of our experimental results. In addition, we extend the analysis to other important materials, Si and Au. We find that the behavior observed experimentally in GaAs is also expected in Si and Au. We also present generalized analytical results for other material systems, which allows us to predict the hardly detectable frequencies. Furthermore, we show that this approach allows access to the materials' acousto-optic coefficients, which are crucial for applications of picosecond ultrasonics.

ACKNOWLEDGMENTS

This work was supported by the German Research Foundation (Deutsche Forschungsgemeinschaft) through the SFB 767. The authors gratefully acknowledge financial support from the China Scholarship Council.

[1] H. Sun, V. A. Stoica, M. Shtein, R. Clarke, and K. P. Pipe, Phys. Rev. Lett. **110**, 086109 (2013).
[2] A. V. Akimov, E. S. K. Young, J. S. Sharp, V. Gusev, and A. J. Kent, Appl. Phys. Lett. **99**, 021912 (2011).
[3] F. Hudert, A. Bruchhausen, D. Issenmann, O. Schecker, R. Waitz, A. Erbe, E. Scheer, T. Dekorsy, A. Mlayah, and J.-R. Huntzinger, Phys. Rev. B **79**, 201307 (2009).
[4] A. Bruchhausen, R. Gebs, F. Hudert, D. Issenmann, G. Klatt, A. Bartels, O. Schecker, R. Waitz, A. Erbe, E. Scheer, J. R. Huntzinger, A. Mlayah, and T. Dekorsy, Phys. Rev. Lett. **106**, 077401 (2011).
[5] M. Schubert, M. Grossmann, C. He, D. Brick, P. Scheel, O. Ristow, V. Gusev, and T. Dekorsy, Ultrasonics **56**, 109 (2015).
[6] J. Cuffe, O. Ristow, E. Chávez, A. Shchepetov, P. O. Chapuis, F. Alzina, M. Hettich, M. Prunnila, J. Ahopelto, T. Dekorsy, and C. M. Sotomayor Torres, Phys. Rev. Lett. **110**, 095503 (2013).
[7] C. He, M. Grossmann, D. Brick, M. Schubert, S. V. Novikov, C. Thomas Foxon, V. Gusev, A. J. Kent, and T. Dekorsy, Appl. Phys. Lett. **107**, 112105 (2015).
[8] A. Bartels, R. Cerna, C. Kistner, A. Thoma, F. Hudert, C. Janke, and T. Dekorsy, Rev. Sci. Instrum. **78**, 035107 (2007).
[9] R. Gebs, G. Klatt, C. Janke, T. Dekorsy, and A. Bartels, Opt. Express **18**, 5974 (2010).
[10] D. E. Aspnes and A. A. Studna, Phys. Rev. B **27**, 985 (1983).
[11] S. Adachi, *GaAs and Related Materials: Bulk Semiconducting and Superlattice Properties* (World Scientific, Singapore, 1994).
[12] C. Thomsen, J. Strait, Z. Vardeny, H. J. Maris, J. Tauc, and J. J. Hauser, Phys. Rev. Lett. **53**, 989 (1984).
[13] C. Thomsen, H. T. Grahn, H. J. Maris, and J. Tauc, Phys. Rev. B **34**, 4129 (1986).
[14] V. Gusev and A. Karabutov, *Laser Optoacoustics* (American Institute of Physics, New York, 1993).
[15] V. Gusev, Acustica Acta Acustica **82**, S37 (1996).
[16] S. A. Akhmanov and V. E. Gusev, Sov. Phys. Usp. **35**, 153 (1992).
[17] V. E. Gusev, Phys. Status Solidi B **158**, 367 (1990).
[18] O. B. Wright and V. E. Gusev, IEEE Trans. Ultrason. Ferroelectr. Freq. Control **42**, 331 (1995).
[19] N. V. Chigarev, D. Y. Parashchuk, Y. S. Pan, and V. É. Gusev, J. Exp. Theor. Phys. **94**, 627 (2002).
[20] P. Babilotte, P. Ruello, D. Mounier, T. Pezeril, G. Vaudel, M. Edely, J. M. Breteau, V. Gusev, and K. Blary, Phys. Rev. B **81**, 245207 (2010).
[21] E. S. K. Young, A. V. Akimov, R. P. Campion, A. J. Kent, and V. Gusev, Phys. Rev. B **86**, 155207 (2012).
[22] W. Chen, H. J. Maris, Z. R. Wasilewski, and S.-I. Tamura, Philos. Mag. B **70**, 687 (1994).
[23] R. Legrand, A. Huynh, B. Jusserand, B. Perrin, and A. Lemaître, Phys. Rev. B **93**, 184304 (2016).
[24] S. M. Avanesyan, V. E. Gusev, and N. I. Zheludev, Appl. Phys. A **40**, 163 (1986).
[25] M. Grossmann, M. Klingele, P. Scheel, O. Ristow, M. Hettich, C. He, R. Waitz, M. Schubert, A. Bruchhausen, V. Gusev, E. Scheer, and T. Dekorsy, Phys. Rev. B **88**, 205202 (2013).
[26] O. B. Wright, B. Perrin, O. Matsuda, and V. E. Gusev, Phys. Rev. B **64**, 081202 (2001).
[27] D. Mirlin, I. Karlik, L. Nikitin, I. Reshina, and V. Sapega, Solid State Commun. **37**, 757 (1981).
[28] J. A. Kash, J. C. Tsang, and J. M. Hvam, Phys. Rev. Lett. **54**, 2151 (1985).

[29] B. P. Zakharchenya, D. N. Mirlin, V. I. Perel', and I. I. Reshina, Sov. Phys. Usp. **25**, 143 (1982).
[30] S. Lyon, J. Lumin. **35**, 121 (1986).
[31] P. Etchegoin, J. Kircher, M. Cardona, C. Grein, and E. Bustarret, Phys. Rev. B **46**, 15139 (1992).
[32] Y. A. Burenkov, Y. M. Burdukov, S. Y. Davidov, and S. P. Nikanorov, Sov. Phys. Solid State **15**, 1175 (1973).
[33] P. Etchegoin, J. Kircher, M. Cardona, and C. Grein, Phys. Rev. B **45**, 11721 (1992).
[34] J. S. Blakemore, J. Appl. Phys. **53**, R123 (1982).
[35] S. Adachi, J. Appl. Phys. **66**, 6030 (1989).
[36] S. Adachi, Phys. Rev. B **35**, 7454 (1987).
[37] P. Etchegoin, J. Kircher, and M. Cardona, Phys. Rev. B **47**, 10292 (1993).
[38] H. M. Lawler, A. Steigerwald, J. Gregory, H. Krzyzanowska, and N. H. Tolk, Mater. Res. Express **1**, 025701 (2014).
[39] S. Adachi, Phys. Rev. B **38**, 12966 (1988).
[40] P. B. Johnson and R. W. Christy, Phys. Rev. B **6**, 4370 (1972).
[41] P. Cheyssac, R. Garrigos, R. Kofman, L. Penavaire, J. Richard, and A. Saïssy, Thin Solid Films **13**, 275 (1972).
[42] D. E. Weiss and L. Muldawer, Phys. Rev. B **10**, 2254 (1974).
[43] Z. Lin, L. V. Zhigilei, and V. Celli, Phys. Rev. B **77**, 075133 (2008).
[44] A. Devos and C. Lerouge, Phys. Rev. Lett. **86**, 2669 (2001).
[45] A. Devos and A. Le Louarn, Phys. Rev. B **68**, 045405 (2003).
[46] A. Devos and R. Côte, Phys. Rev. B **70**, 125208 (2004).
[47] C. Rossignol, J. M. Rampnoux, T. Dehoux, S. Dilhaire, and B. Audoin, Rev. Sci. Instrum. **77**, 033101 (2006).
[48] A. Devos, Ultrasonics **56**, 90 (2015).
[49] V. V. Temnov, C. Klieber, K. A. Nelson, T. Thomay, V. Knittel, A. Leitenstorfer, D. Makarov, M. Albrecht, and R. Bratschitsch, Nat. Commun. **4**, 1468 (2013).
[50] K. J. Manke, A. A. Maznev, C. Klieber, V. Shalagatskyi, V. V. Temnov, D. Makarov, S.-H. Baek, C.-B. Eom, and K. A. Nelson, Appl. Phys. Lett. **103**, 173104 (2013).
[51] O. Matsuda, M. C. Larciprete, R. Li Voti, and O. B. Wright, Ultrasonics **56**, 3 (2015).